Lifetime and hfs of the $(5s5p)\,{}^1P_1$ State of Cadmium*

ALLEN LURIO
IBM Watson Laboratory, Columbia University, New York, New York

AND

ROBERT NOVICK†
Columbia Radiation Laboratory, Columbia University, New York, New York

(Received 12 September 1963)

The lifetime and hfs of the $(5s5p)\,{}^1P_1$ state of cadmium have been measured by the level crossing technique. Coherence narrowing of the zero-field level crossing (Hanle effect) signal has been observed and found to be in agreement with Barrats theory. The lifetime obtained from two independent experiments is $1.66\pm0.05\times10^{-9}$ sec. This value is considerably smaller than earlier values. The ratio of this lifetime to the $(5s5p)\,{}^3P_1$ state lifetime obtained by Byron *et al.* is $6.95\pm0.30\times10^{-4}$—in good agreement with the results of Filippov and Kuhn. The dipole interaction constant $A({}^1P_1)$ obtained for Cd^{111} is $|A({}^1P_1)|=186\pm4$ Mc/sec. This result is compared to that obtained by Heydenburg. Using the present lifetime measurement and the known hfs intervals for the $^3P_2$ and $^3P_1$ states we find for the theoretical value of this constant $A({}^1P_1)=-152\pm25$ Mc/sec. The single electron hfs constants for the $(5s5p)$ configuration are tabulated.

INTRODUCTION

THIS is the first paper of a series in which we report on the determination of the lifetime of the first excited $^1P_1$ states of the group II elements by the zero-field level crossing method. Zero-field level crossing is also referred to in the literature as the Hanle effect and the magnetic depolarization of resonance radiation.[1] In the 1930's when this technique was first employed the phenomenon of coherence narrowing[2] was not known. We believe some of the earlier results may be in error because proper allowance was not made for this effect. Radiation trapping and the resulting coherence narrowing increase the apparent lifetime of the atomic states. Improvement in experimental technique such as more sensitive photomultipliers, high transmittance interference filters and more intense light sources permit one to make observations at very much lower vapor densities where the effects of radiation trapping can be demonstrated to be negligible. In addition, the theory of Barrat[2] permits one to extrapolate the observations to zero density. The earlier observations were made by observing the polarization of the fluorescence with dc detection techniques. In order to overcome the effects of instrumental scattering and the inherent losses in polarizers, the early experiments were performed at such high vapor densities that radiation trapping was almost certainly occurring.

We present in this paper[3] the measurement of the lifetime of the $(5s5p)\,{}^1P_1$ state of Cd and hfs separation of the $^1P_1$ state of Cd^{111}. In Fig. 1 is shown the term structure of the ground- and lowest excited-state configuration $(5s5p)$ of Cd. The wavelength of the resonance radiation connecting $^1S_0$ and the $^1P_1$ states is 2288 Å. In order to fully test for the effects of radiation trapping we performed two different experiments. We first determined the lifetime of a sample of atoms contained in a small quartz cell. The vapor density in the cell could be readily increased by heating so that the effects of coherence narrowing could be studied quantitatively. As a check on the extrapolation of these results to zero vapor density we undertook a second experiment on an atomic beam of cadmium atoms. In the case of the beam it was possible to eliminate most of the instrumental scattering and thereby obtain observations at lower densities. The experimental simplicity and reproducibility of the results indicate that the

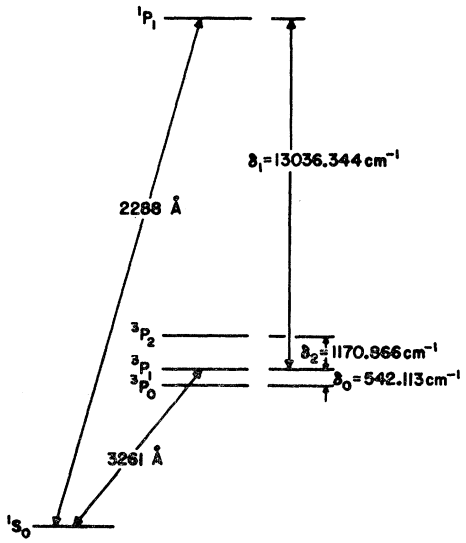

FIG. 1. Term structure of low-lying levels of Cd.

* Work supported in part by the U. S. Air Force Office of Scientific Research under Grant No. AF-AFOSR-62-65 and in part by the Joint Services (U. S. Army, Office of Naval Research, and Air Force Office of Scientific Research).

† Alfred P. Sloan Foundation Fellow.

[1] For a general survey of the earlier work see A. Mitchell and M. Zemansky, *Resonance Radiation and Excited Atoms* (Cambridge University Press, New York, 1961); and P. Pringsheim *Fluorescence and Phosphorescence* (Interscience Publishers, Inc., New York, 1949).

[2] J. P. Barrat, J. Phys. Radium **20**, 541, 633, 657 (1959).

[3] Some preliminary results of this work has appeared earlier: A. Lurio and R. Novick, Bull. Am. Phys. Soc. **7**, 258 (1962).

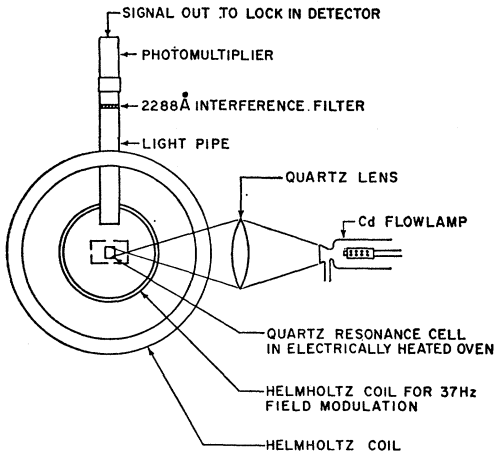

FIG. 2. Schematic diagram of the cell apparatus.

method will yield more reliable lifetime measurements than other techniques which require a knowledge of the density of the scattering atoms.

The lifetime of the $^1P_1$ state is of interest for several reasons: (1) From $\tau(^1P_1)$ and $\tau(^3P_1)$ one obtains the intermediate coupling constants c_1 and c_2 for the electronic configuration (sp); (2) the results may be used as a test of wave functions calculated for this configuration or as a test for approximation methods used to calculate oscillator strengths; and (3) the lifetimes are useful in the astrophysical interpretation of some nebular lines.[4]

APPARATUS

As indicated above, two different apparatus were used in obtaining the data. In both arrangements the direction of the incident light, the direction of the applied magnetic field, and the direction of observation were mutually orthogonal.

In Fig. 2 is shown a schematic diagram of the cell apparatus. The light source which will be described in another publication is a modification of the Cario Lochte-Holtgreven flow lamp that when focused with an $f/1.5$ optical system gave an intensity over a $\frac{3}{8}$-in.-diam region of 400μW in about two Doppler widths. The quartz resonance cells were cylinders approximately 1 in. in diameter and $\frac{3}{8}$ in. long. They were placed in an electrically heated oven with bifilar windings. The scattered light was focused into an aluminized light pipe at the far end of which was a 2288-Å interference filter and a Dumont No. 7664 photomultiplier tube. This enabled one to remove the photomultiplier from the magnetic field region. In addition to the Helmholtz coils which produced the dc magnetic field at the cell, there was a second set of coils which were modulated at 37 cps. The photomultiplier output was fed into a lock-in amplifier and that component of the signal in phase with the 37-cps modulating field was detected. This signal was presented on a recorder as the dc magnetic field was slowly swept over a region of about 300 G symmetrically located about zero field. The amplitude of the modulating field was small enough so that modulation broadening amounted to only a few percent.

In Fig. 3 is shown a schematic diagram of the apparatus used for the atomic beam experiment. The only difference in the incident optics of Fig. 3 compared to Fig. 2 is the addition of a pile-of-quartz-plates linear polarizer. A pile of 6 plates gave a polarization of about 55% at 2288 Å and only attenuated the desired component of the light beam by about 40%. The beam source is a stainless steel oven located about 4 in. below the scattering region. The beam effuses through a $\frac{1}{4}$-in.-diam crinkle foil[5] aperture at the top of the oven and is further collimated into a $\frac{1}{2}$-in.-diam region as it passes vertically through the scattering chamber. After passing through the scattering region the beam is collected on a liquid N_2 trap. A beam flag is provided to aid in aligning the optics and to determine the amount of instrumental scattering in the absence of the beam. Under operating conditions the instrumental scattering can be reduced to several times the dark current of the photomultiplier while the beam scattered resonance radiation can easily be made 100 times the dark current. In this arrangement the dc scattered resonance radiation signal is collected by an aluminized light pipe, passed through a 2288-Å interference filter and detected by a Dumont No. 7664 photomultiplier. The photomultiplier output is further amplified by a HP 412A vacuum tube voltmeter and presented on a servo recorder. Data are taken by observing the recorder signal as the static magnetic field is swept manually from $+H$ to $-H$ at fixed field intervals. In both experimental arrangements care must be taken to adjust the optics such that the recorded curves are

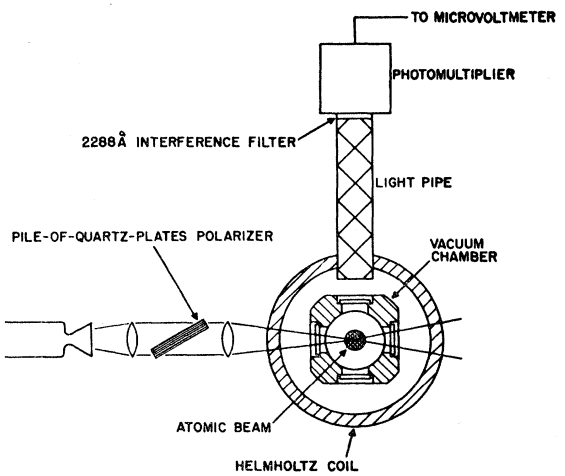

FIG. 3. Schematic diagram of the atomic beam apparatus.

[4] R. H. Garstang, J. Opt. Soc. Am. **52**, 845 (1962).

[5] *Electronics and Electron Physics*, edited by L. Marton (Academic Press Inc., New York, 1956), Vol. VIII, p. 19.

symmetrical with respect to plus and minus field directions. In this experiment we were able to work at lower densities than in the cell measurements for two reasons: (1) the instrumental scattering can be reduced by an order of magnitude in this case since the entrance and exit windows are now well separated from the scattering atoms and (2) the data are taken by observing the direct scattering (no field modulation) so we can observe the full signal and are not limited to a fraction of the available intensity of a modulation experiment by the requirement of small modulation amplitude to avoid distortion of the line shape.

THEORY

The stable isotopes of Cd have either spin zero or spin $\frac{1}{2}$. We shall treat the case of spin $\frac{1}{2}$ since by letting the $^1P_1$ state dipole interaction constant $A(^1P_1)$ go to zero we can obtain the result for spin zero. The x axis is taken to be antiparallel to the direction of propagation of the incident light and the z axis to be along the static magnetic field. We must now express the magnetic field dependence of the scattered resonance radiation in terms of the lifetime and dipole interaction constant $A(^1P_1)$. The expression for the rate of coherent scattering of light has been given by Breit, Franken and others[6] and is

$$R \propto N \sum_{\substack{\mu\mu' \\ mm'}} \frac{f_{\mu m} f_{m\mu'} g_{\mu' m'} g_{m'\mu}}{\Gamma - i(E_\mu - E_{\mu'})/\hbar}, \tag{1}$$

where $f_{\mu m}=(\mu|\mathbf{f}\cdot\mathbf{r}|m)$, $g_{\mu m}=(\mu|\mathbf{g}\cdot\mathbf{r}|m)$, $\Gamma=1/\tau$, and τ is the lifetime of the excited state.

In the application of this formula the dependence of the matrix elements of $\mathbf{f}\cdot\mathbf{r}$ and $\mathbf{g}\cdot\mathbf{r}$ on the external magnetic field must be taken into account. It is known that for arbitrary J and $I=\frac{1}{2}$ the magnetic field dependence of the wave functions $|H,F,m\rangle$ can be expressed in terms of the zero-field wave functions $|0,F,m\rangle$ by the relation

$$|H, J\pm\tfrac{1}{2}, m\rangle = A_\pm|0, J+\tfrac{1}{2}, m\rangle + B_\pm|0, J-\tfrac{1}{2}, m\rangle, \tag{2}$$

where

$$A_\pm = \frac{1}{\sqrt{2}}\left[1\pm\frac{1-2mx/(2J+1)}{[1-4mx/(2J+1)+x^2]^{\frac{1}{2}}}\right]^{1/2},$$
$$B_\pm = \mp\frac{1}{\sqrt{2}}\left[1\mp\frac{1-2mx/(2J+1)}{[1-4mx/(2J+1)+x^2]^{\frac{1}{2}}}\right]^{1/2}, \tag{3}$$

and

$$x=\frac{(g_J+g_I)\mu_0 H}{A(J+1/2)}.$$

Also we have for this case

$$E_{J\pm1/2,m} = E_0 + mg_J\mu_0 H - \tfrac{1}{4}A \pm \tfrac{1}{4}A(2J+1) \times[1-4mx/(2J+1)+x^2]^{1/2}. \tag{4}$$

After some tedious algebra we obtain for the scattering rate at the spherical coordinate angles θ, φ (θ is the polar angle),

$$I_\pi = kP^2\left\{\frac{2\sin^2\theta}{9\Gamma}+\frac{4-6\sin^2\theta}{9\Gamma}\left(\frac{1}{\Delta_+^2}+\frac{1}{\Delta_-^2}\right)+\frac{\Gamma}{9}(6\sin^2\theta-4)\left[\frac{1/\Delta_+^2}{\Gamma^2+(E_{\frac{3}{2},-\frac{1}{2}}-E_{\frac{1}{2},-\frac{1}{2}})^2/\hbar^2}+\frac{1/\Delta_-^2}{\Gamma^2+(E_{\frac{3}{2},\frac{1}{2}}-E_{\frac{1}{2},\frac{1}{2}})^2/\hbar^2}\right]\right\}, \tag{5}$$

$$\begin{aligned} I_\sigma = kP^2\Bigg\{&\frac{2-\sin^2\theta}{\Gamma}+\frac{3\sin^2\theta-2}{9\Gamma}\left(\frac{1}{\Delta_+^2}+\frac{1}{\Delta_-^2}\right)+\frac{\Gamma}{9}(2-3\sin^2\theta)\left[\frac{1/\Delta_+^2}{\Gamma^2+(E_{\frac{3}{2},-\frac{1}{2}}-E_{\frac{1}{2},-\frac{1}{2}})^2/\hbar^2}+\frac{1/\Delta_-^2}{\Gamma^2+(E_{\frac{3}{2},\frac{1}{2}}-E_{\frac{1}{2},\frac{1}{2}})^2/\hbar^2}\right] \\ &+\frac{\frac{1}{4}[1-(\frac{1}{3}+x)/\Delta_+][\Gamma\cos2\phi-(1/\hbar)(E_{\frac{3}{2},\frac{3}{2}}-E_{\frac{3}{2},-\frac{1}{2}})\sin2\phi]\sin^2\theta}{\Gamma^2+(E_{\frac{3}{2},\frac{3}{2}}-E_{\frac{3}{2},-\frac{1}{2}})^2/\hbar^2} \\ &+\frac{\frac{1}{4}[1+(\frac{1}{3}+x)/\Delta_+][\Gamma\cos2\phi-(1/\hbar)(E_{\frac{3}{2},\frac{3}{2}}-E_{\frac{1}{2},-\frac{1}{2}})\sin2\phi]\sin^2\theta}{\Gamma^2+(E_{\frac{3}{2},\frac{3}{2}}-E_{\frac{1}{2},-\frac{1}{2}})^2/\hbar^2} \\ &+\frac{\frac{1}{4}[1-(\frac{1}{3}-x)/\Delta_-][\Gamma\cos2\phi-(1/\hbar)(E_{\frac{3}{2},\frac{1}{2}}-E_{\frac{3}{2},-\frac{3}{2}})\sin2\phi]\sin^2\theta}{\Gamma^2+(E_{\frac{3}{2},\frac{1}{2}}-E_{\frac{3}{2},-\frac{3}{2}})^2/\hbar^2} \\ &+\frac{\frac{1}{4}[1+(\frac{1}{3}-x)/\Delta_-][\Gamma\cos2\phi+(1/\hbar)(E_{\frac{3}{2},-\frac{3}{2}}-E_{\frac{1}{2},\frac{1}{2}})\sin2\phi]\sin^2\theta}{\Gamma^2+(E_{\frac{3}{2},-\frac{3}{2}}-E_{\frac{1}{2},\frac{1}{2}})^2/\hbar^2}\Bigg\}, \end{aligned} \tag{6}$$

where I_π is the intensity of the scattered resonance radiation arising from the π component of the incoming light; I_σ is the intensity of the scattered resonance radiation arising from the σ component of the incoming light; $\Delta_\pm=(1\pm(2x/3)+x^2)^{1/2}$; and k is a geometrical factor. These expressions give the general result for the observation direction at spherical coordinate angle θ and φ but we take $\varphi=\pi/2$ and $\theta=\pi/2$ for our experimental arrangement. In the case of $I=0$ we will have

[6] G. Breit, Rev. Mod. Phys. **5**, 91 (1933); P. Franken, Phys. Rev. **121**, 508 (1961); M. E. Rose and R. L. Carovillano, Phys. Rev. **122**, 1185 (1961).

$x \rightarrow \infty$ and $\Delta_\pm \rightarrow x$. Then we obtain

$$I_\pi = kP^2(2\sin^2\theta/\Gamma), \tag{7}$$

$$I_\sigma = kP^2\left[\frac{1}{\Gamma} + \frac{\Gamma\cos 2\varphi + 2(g_J\mu_0 H)\sin 2\varphi}{\Gamma^2 + 4(g_J\mu_0 H)^2}\sin^2\varphi\right]. \tag{8}$$

RESULTS

A. Cell Experiment

To obtain the $^1P_1$ state lifetime, a cell containing more than 99% even isotopes ($I=0$) was prepared from an enriched sample received from the Oak Ridge

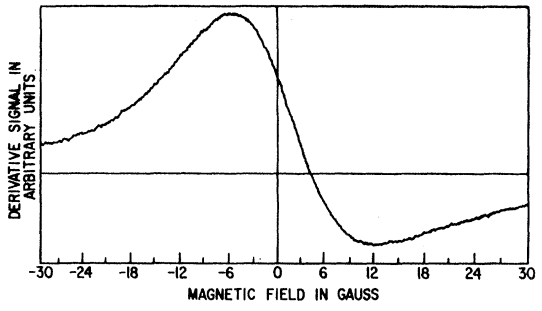

FIG. 4. Derivative line shape curve obtained at high density with zero nuclear spin isotopes.

National Laboratory (see Fig. 2). The positive and negative field portions of the trace should be antisymmetric if the trace is the derivative of a Lorentzian curve. These portions of the curve, however, are not exactly antisymmetric and this is most likely due to the fact that the incident and exitant optics were not exactly perpendicular to each other. This asymmetry is not due to the direction in which the field is swept since at each cell temperature the average of two curves was taken in which the field was swept oppositely with time. At high temperatures where coherence narrowing becomes appreciable, severe distortion of the antisymmetric resonance curves occurred. This is caused by the attenuation of the incident light by the atoms. The effect of the attenuation is to produce more scattering from atoms in the front part of the cell than in the rear so that even though the incident and exitant optics are exactly perpendicular, the effective angle of scattering is greater than 90°. In Appendix I, we give a first-order theory to account for this effect. This theory explains the data well enough so that even severely distorted curves as in Fig. 4 can be interpreted with confidence. In Fig. 5 is shown the apparent lifetime versus the density of atoms in the scattering cell. This curve illustrates the phenomenon of coherence narrowing which has been explained by Barrat. The extrapolated intercept of the curve at zero density is the true lifetime of the state. This value is $1.66\pm0.05\times10^{-9}$ sec.

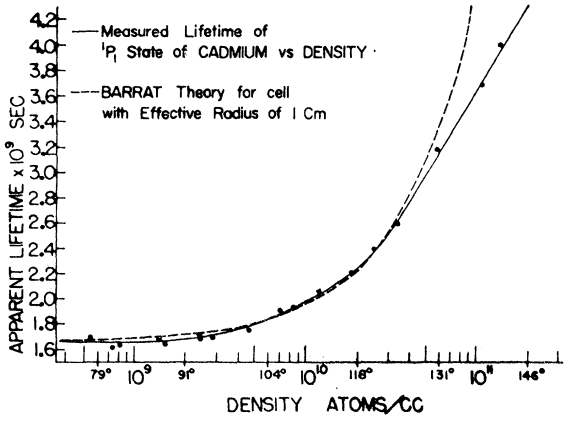

FIG. 5. Apparent lifetime versus density (small figures on the abscissa refer to the cell temperature).

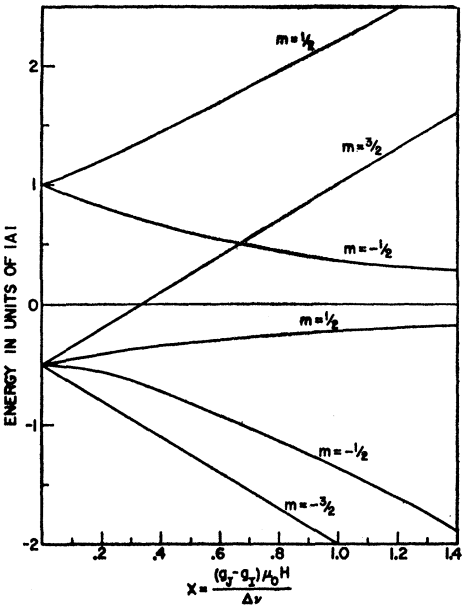

FIG. 6. Energy level diagram of the $^1P_1$ state of Cd^{111} and Cd^{113}.

In Fig. 6 is shown the hfs of the $^1P_1$ state with A assumed negative. From this figure we see that the

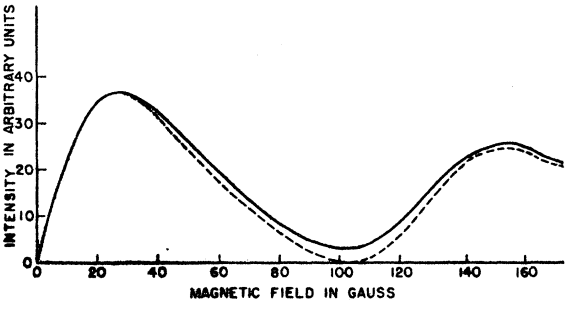

FIG. 7. Solid line is derivative line shape curve obtained with cell containing 92% Cd^{111}. Dashed line is theoretical curve calculated for 92% Cd^{111}, 8% even isotopes, $\tau(^1P_1)=1.66\times10^{-9}$ sec, $A(^1P_1)=187$ Mc/sec and unpolarized incident light.

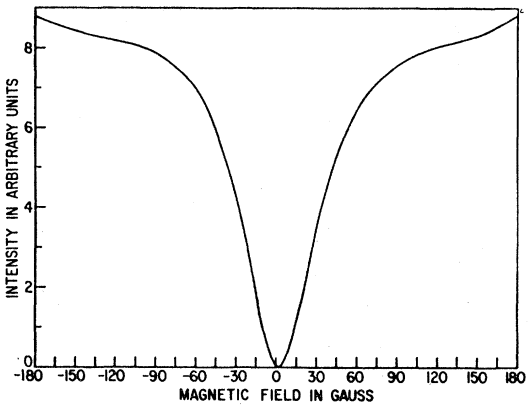

FIG. 8. Field dependence of the intensity of the light scattered from a beam of natural cadmium atoms.

$F=\frac{3}{2}$, $m=\frac{3}{2}$ level and the $F=\frac{1}{2}$, $m=-\frac{1}{2}$ level cross at $x=\frac{2}{3}$. This level crossing will result in an intensity change in the scattered resonance radiation from which the hfs separation may be determined. To within the accuracy of the present experiment we can take $g_J(^1P_1)$ to be 1.00. One should note that one cannot determine the sign of A from the level crossing at $x=\frac{2}{3}$ since if A were positive, the $F=\frac{3}{2}$, $m=-\frac{3}{2}$ and the $F=\frac{1}{2}$, $m=\frac{1}{2}$ levels would cross at the same value of x.

In Fig. 7 is shown the zero-field and high-field level crossing derivative signal taken with a cell containing 92% Cd^{111} and 8% even isotope. Plotted with the experimental curve (the average of several runs at the same temperature) is a theoretical curve for $A(^1P_1)=187$ Mc/sec, where the ratio of Cd^{111} to the even isotopes is taken to be 92:8. The theoretical curve is normalized to the experimental curve at $x=0.14$. From a family of such theoretical curves for different values of $A(^1P_1)$ and several experimental line shapes we find that $|A(^1P_1)|=186\pm4$ Mc/sec. We believe that the failure to obtain agreement in the amplitude of the high-field crossing may be due to either (1) the isotopic abundance analysis given by ORNL is in error or (2) coherence narrowing changes the relative amplitude of the two peaks. In either case the shape of the curve (i.e., the location of the peak and dip) is independent of over-all amplitude and hence should not lead to any error in A.

B. Atomic Beam

Natural cadmium was used in the oven for the atomic beam zero-field level crossing experiment, hence in interpreting the data one must allow for the effect of the 25% of odd isotopes. From the cell experiments on Cd^{111} the hfs of the odd isotopes is known so that their effect can be calculated. In Fig. 8 is shown an experimental curve of the scattered light intensity I as a function of the magnetic field. At all beam densities used, the curves were symmetric about zero field. The effect of the odd isotopes is most pronounced in the curve of Fig. 8 in the wings where the high-field level crossing occurs ($H=122$ G). At the highest beam densities used, a factor of 30 over the minimum density, a narrowing of about 3% was found. The average of 8 runs taken on five different days gives $\tau(^1P_1)=1.66\pm0.06\times10^{-9}$ sec.

TABLE I. Tabulation of present and earlier results for the lifetime of the Cd($5s5p$ $^1P_1$ and $^3P_1$ state.

Author	Measurement	Result
Kuhn[a]	$\tau(^1P_1)$	2×10^{-9} sec
	$\tau(^1P_1)/\tau(^3P_1)$	$7.8\pm1.1\times10^{-4}$
Zemansky[b]	$\tau(^1P_1)$	1.99×10^{-9} sec
Filippov[c]	$\tau(^1P_1)/\tau(^3P_1)$	$7.24\pm0.28\times10^{-4}$
Webb and Messenger[d]	$\tau(^1P_1)$	$\approx2\times10^{-9}$ sec
Present work	$\tau(^1P_1)$	$1.66\pm0.05\times10^{-9}$ sec
Byron *et al.*[e]	$\tau(^3P_1)$	$2.39\pm0.04\times10^{-6}$ sec
Ratio of above two results	$\tau(^1P_1)/\tau(^3P_1)$	$6.95\pm0.30\times10^{-4}$

[a] W. Kuhn, Kgl. Danske Videnskab. Selskab, Mat.-Fys. Medd. **1**, 12 (1926).
[b] M. Zemansky, Z. Physik **72**, 587 (1931).
[c] A. Filippov, Physik Z. Sowjetunion **1**, 289 (1932).
[d] H. W. Webb and H. A. Messenger, Phys. Rev. **66**, 77 (1944).
[e] See Ref. 7.

DISCUSSION OF RESULTS

Table I shows the present and previous results for the lifetime of the $^1P_1$ state and the best value for the lifetime of the $^3P_1$ state. Our value for $\tau(^1P_1)$ is considerably lower than values obtained previously. We do not know the reason for this discrepancy but the results obtained by the first three experimenters listed in Table I all depended on an accurate knowledge of

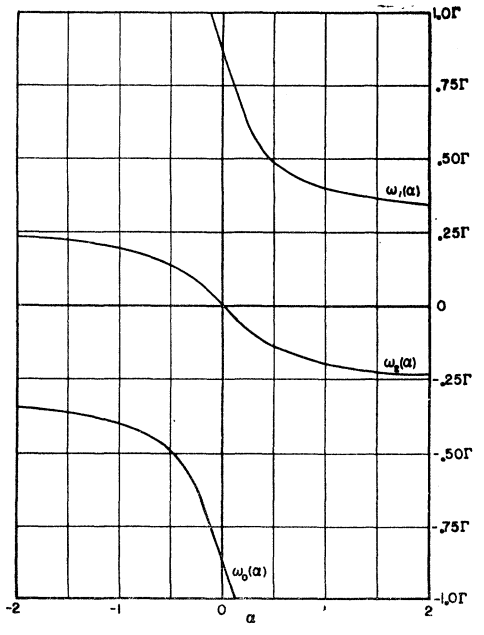

FIG. 9. Location of the extrema of the derivative line shape curve as a function of α where $\alpha=\frac{1}{2}\langle\cos2\varphi\rangle_{av}/\langle\sin2\varphi\rangle_{av}$ and φ is the mean scattering angle in the plane defined by the incident light and observation directions.

TABLE II. Experimental and derived results necessary to calculate $A(^1P_1)$.[a]

	Cd^{111}	Cd^{113}
Fractional abundance	12.75%	12.16%
g_I	$+64.80(1)\times10^{-5}$	$67.78(1)\times10^{-5}$
$\Delta\nu(^3P_1)$	6185.72(2) Mc/sec	6470.79(2) Mc/sec
$\Delta\nu(^3P_2)$	8232.341(2) Mc/sec	8611.586(4) Mc/sec
a_s	$-12.393(33)\times10^3$ Mc/sec	$-12.963(35)\times10^3$ Mc/sec
$a_{1/2}$	$-1.672(71)\times10^3$ Mc/sec	$-1.749(75)\times10^3$ Mc/sec
$a_{3/2}$	$-0.259(11)\times10^3$ Mc/sec	$-0.271(12)\times10^3$ Mc/sec
ξ	1.034	1.034

[a] See Ref. 9 for the definition of the symbols used in this table.

the Cd vapor density which is difficult to measure reliably. Using the Byron, McDermott, and Novick[7] value for $\tau(^3P_1)$ and our value for $\tau(^1P_1)$ we obtain a lifetime ratio $\tau(^1P_1)/\tau(^3P_1)=6.95\pm0.30\times10^{-4}$ which is in good agreement with the results of Filippov and of Kuhn. This is to be expected since the lifetime ratio obtained by the methods of Filippov or Kuhn is more reliable than Kuhn's absolute lifetime value. The lifetime calculated by the method of Bates and Damgaard[8] gives 1.62×10^{-9} sec which is in surprisingly good agreement with our value.

One of the most important results to be obtained from these lifetimes is the intermediate coupling coefficients α and β or c_1 and c_2 which are defined by Lurio, Mandel, and Novick.[9] Taking $\tau(^1P_1)=1.66\times10^{-9}$ sec and $\tau(^3P_1)=2.39\times10^{-6}$ sec, we find[10] $\alpha=0.9990$, $\beta=-0.0448$, $c_1=0.5402(8)$, and $c_2=0.8415(6)$. With these results for the coupling coefficients and the quantities given in Table II we may compute the $^1P_1$ state hfs from the formula,[9]

$$A(^1P_1)=a_s[(c_1^2/2)-(c_2^2/4)]+a_{3/2}(5/4)c_2^2+a_{1/2}(c_2^2/2)+2c_1c_2(5\xi a_{3/2}/16\sqrt{2}). \quad (9)$$

We find for Cd^{111}, $A(^1P_1)=-152\pm25$ Mc/sec. This value is to be compared with the experimental result $|A(^1P_1)|=186\pm4$ Mc/sec. In the calculation of $A(^1P_1)$ from Eq. (9) the s and p electron contributions are of comparable size but of opposite sign. In view of this cancellation of terms in the expression for $A(^1P_1)$ we feel that the agreement between experiment and theory is quite good, provided of course that $A(^1P_1)$ is negative. Unfortunately, we have not been able to determine experimentally the sign of $A(^1P_1)$.

The corresponding $A(^1P_1)$ for Cd^{113} is directly obtained from the known magnetic moment ratio.[11] The average $A(^1P_1)$ for both odd isotopes has been measured by Heydenburg who finds $\langle A(^1P_1)\rangle_{av}=242$ Mc/sec. The reason for the discrepancy between this result and our value is not known but it is perhaps significant that Heydenburg[12] found a 2.6:1 even to odd isotope ratio from his experiment whereas the presently accepted value for the ratio is 3.00:1.

APPENDIX I

Analysis of Mixed Lorentzian and Dispersion-Shaped Curves

The expression for the intensity of the scattered resonance radiation from the $I=0$ spin isotopes is given by Eqs. (7) and (8). Experimentally we choose $\theta=\pi/2$ and $\varphi=\pi/2$ as carefully as possible; however, the two effects discussed previously in the results section can lead to effective values of θ and φ being slightly different from $\pi/2$. If θ is not exactly $\pi/2$ no distortion of the resonance curve occurs, since the magnetic field-dependent part of the scattered light intensity is only reduced in intensity by the $\sin^2\theta$ factor. For $\varphi\neq\pi/2$, however, the Lorentzian line shape is distorted by the addition of a dispersion-shaped line. In Eq. (8) let us replace $\cos2\varphi$ and $\sin2\varphi$ by the appropriate average value, that is, by $\langle\cos2\varphi\rangle_{av}$ and $\langle sin2\varphi\rangle_{av}$. Then for unpolarized incident light and $\theta=\pi/2$,

$$I=I_0\frac{3}{\Gamma}+2I_0\langle\sin2\varphi\rangle_{av}\frac{\alpha\Gamma+\omega}{\Gamma^2+4\omega}, \quad (10)$$

where $\alpha=\frac{1}{2}\langle\cos2\varphi\rangle_{av}/\langle\sin2\varphi\rangle_{av}$ and $\omega=g_J\mu_0H$. From this expression we see that if we detect I versus H then $[I(+H)+I(-H)]/2$ is a pure Lorentzian curve and $[I(+H)-I(-H)]/2$ is a pure dispersion curve and the parameter of interest Γ can be obtained unambiguously.

If one is using field modulation so that $\partial I/\partial H$ versus H is detected, then a different procedure must be used. Our detected signal is now

$$\frac{\partial I}{\partial H}=2I_0\langle\sin2\varphi\rangle_{av}\frac{\Gamma^2-8\omega\Gamma\alpha-4\omega^2}{(\Gamma^2+4\omega^2)^2}. \quad (11)$$

In general, the data are obtained under conditions where $\alpha\gg1$ (i.e., where $\bar{\varphi}\gtrsim90°$) so we will have a curve with a maxima and a minima almost equally spaced

[7] B. Byron, M. N. McDermott, and R. Novick, following paper, Phys. Rev. **134**, A615 (1964).
[8] D. R. Bates and A. Damgaard, Phil. Trans. Roy. Soc. (London) **A 242**, 101 (1949).
[9] A. Lurio, M. Mandel, and R. Novick, Phys. Rev. **126**, 1758 (1962).
[10] The sign of β is determined from the fine structure splitting, see G. Breit and L. A. Wills, Phys. Rev. **44**, 470 (1933).
[11] W. G. Proctor and F. C. Yu, Phys. Rev. **76**, 1728 (1949).
[12] N. P. Heydenburg, Phys. Rev. **43**, 640 (1933).

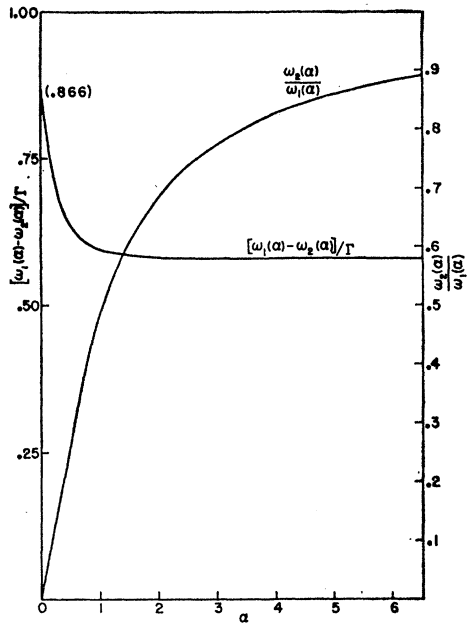

FIG. 10. Ratio and difference of the two extrema nearest $H=0$ as a function of α.

about $H=0$ and a third very shallow extrema far from $H=0$. To find where these extrema occur, we use the usual condition, $(\partial/\partial\omega)(\partial I/\partial H)=0$. This leads to the cubic equation

$$\omega^3+3\omega^2\Gamma\alpha-\tfrac{3}{4}\omega\Gamma^2-\tfrac{1}{4}\Gamma^3\alpha=0. \tag{12}$$

This equation has three real roots independent of the sign of α which are given by the expression

$$\omega=\Gamma(1+4\alpha^2)^{1/2}\cos(\tfrac{1}{3}\Phi+K120°)-\alpha\Gamma \quad K=0,\,1,\,2, \tag{13}$$

with

$$\Phi=\cos^{-1}\frac{-2\alpha}{(1+4\alpha^2)^{1/2}}=180°-\tan^{-1}(1/2\alpha), \quad \alpha>0, \tag{14}$$
$$=\tan^{-1}(1/2|\alpha|), \qquad \alpha<0.$$

Also we have $\omega_0(\alpha)=-\omega_1(-\alpha)$, $\omega_1(\alpha)=-\omega_0(-\alpha)$ and $\omega_2(\alpha)=-\omega_2(-\alpha)$, where 0, 1, and 2 go with the values of K in Eq. (13). For $\alpha>2$ we may approximate the roots to better than 1% by the relations

$$\omega_0=-3\alpha\Gamma-\Gamma/4\alpha,$$
$$\omega_1=\Gamma\left(\frac{\sqrt{3}}{6}+\frac{1}{9\alpha}+\frac{\sqrt{3}}{162\alpha^2}\right), \tag{15}$$
$$\omega_2=\Gamma\left(\frac{\sqrt{3}}{6}-\frac{1}{9\alpha}+\frac{\sqrt{3}}{162\alpha^2}\right).$$

For $|\alpha|<2$ the value of the roots is shown in Fig. 9. The most important conclusion from this analysis is that if $|\alpha|>2$, the difference between the two extrema near $H=0$ is independent of α to within 1% since

$$\omega_1-\omega_2=\frac{\Gamma}{\sqrt{3}}+\frac{\sqrt{3}\Gamma}{81\alpha^2}. \tag{16}$$

The difference between these two extrema for $|\alpha|<2$ is also shown in Fig. 10.

α may be determined from the experimental measured values of H at the two extrema since

$$f(\alpha)=-\frac{\omega_2(\alpha)}{\omega_1(\alpha)}=-\frac{\omega_2(-\alpha)}{\omega_0(-\alpha)}$$
$$=-\frac{[1+4\alpha^2\cos(\tfrac{1}{3}\Phi+300)-\alpha]^{1/2}}{[1+4\alpha^2\cos(\tfrac{1}{3}\Phi+60)-\alpha]^{1/2}} \tag{17}$$

and $f(\alpha)$ is plotted versus α in Fig. 10.

The theory may be tested by determining from the experimental curves where the signal does through its zero value near $H=0$. This value is given by the equation

$$\omega^2+2\omega\Gamma\alpha-\tfrac{1}{4}\Gamma^2=0, \tag{18}$$

with the solution near $H=0$ being

$$\omega=-\alpha\Gamma+\tfrac{1}{2}\Gamma(1+4\alpha^2)^{1/2}.$$

This crossing value is thus determined by α and Γ which have been obtained from ω_1 and ω_2 and must be determined by these values for the theory to apply.